

Record-breaking climate anomalies lead to severe drought and environmental disruption in western Patagonia in 2016

R. D. Garreaud^{1,2,*}

¹Department of Geophysics, and ²Center for Climate and Resilience Research Universidad de Chile, Blanco Encalada 2002, Santiago, Chile

ABSTRACT: Traditionally a temperate and hyper-humid region, western Patagonia experienced its most severe drought during the summer and fall of 2016. Along with precipitation deficits larger than 50 % there was a similar reduction in river discharge into coastal waters, a decline in vegetation productivity, excessive solar radiation at the surface, and frequent upwelling-favorable wind events offshore. The combination of these regional-scale anomalies seems to have set the stage for environmental disturbances that, although not new in western Patagonia, occurred with unprecedented magnitude, including severe urban air pollution episodes, large forest fires, and the worst ever recorded harmful algae bloom (HAB). The local climate anomalies were in turn related to the concomitant strong El Niño (through atmospheric teleconnections) and, to a lesser extent, anthropogenic climate change mediated by the positive polarity of the Southern Annular Mode (SAM) and internal variability, as both modes weakened the westerlies. Drier than present conditions are consistently projected for northern Patagonia during the 21st century as a consequence of anthropogenic increases in radiative forcing; superposition of El Niño events in this altered climate may result in a higher frequency of extreme droughts and environmental disruptions like those observed in 2016.

KEY WORDS: ENSO · Southern Annular Mode · SAM · Climate change · Patagonia · Environment · Harmful algal bloom · HAB

Resale or republication not permitted without written consent of the publisher

1. INTRODUCTION

Western Patagonia—the narrow strip of land between the Pacific and the Austral Andes (Fig. 1a)—features a temperate, hyper-humid climate, thus hosting massive freshwater reserves in its glaciers and ice fields, an intricate network of rivers and fjords, and a high degree of endemic biodiversity (e.g. Martínez-Harms & Gajardo 2008). Copious precipitation ($>3000 \text{ mm yr}^{-1}$) in that region is delivered year-round by the frequent arrival of mid-latitudes storms (e.g. Garreaud et al. 2009), embedded in the Southern Hemisphere (SH) westerly wind belt, further enhanced by orographic uplift over the western side of the Andes (Paruelo et al. 1998, Smith & Evans

2007, Viale and Garreaud 2015). Given its nature, precipitation variability over western Patagonia is tightly coupled with changes in the intensity of the low-level westerly winds impinging the austral Andes (Garreaud 2007, Montecinos et al. 2011, Garreaud et al. 2013) that raises to $\sim 1500 \text{ m}$ above mean sea level (MSL) in these latitudes. The flow is in turn coupled with the mass field (e.g. sea level pressure [SLP] anomalies) over the southeast Pacific and modulated by large-scale modes of atmospheric circulation, namely the El Niño-Southern Oscillation (ENSO) and the Southern Annular Mode (SAM) (e.g. Schneider & Gies 2004, Gillett et al. 2006, Garreaud et al. 2009, Silvestri & Vera 2009). Nonetheless, the ENSO/SAM combined effect has not been docu-

*Corresponding author: rgarraeu@dgf.uchile.cl

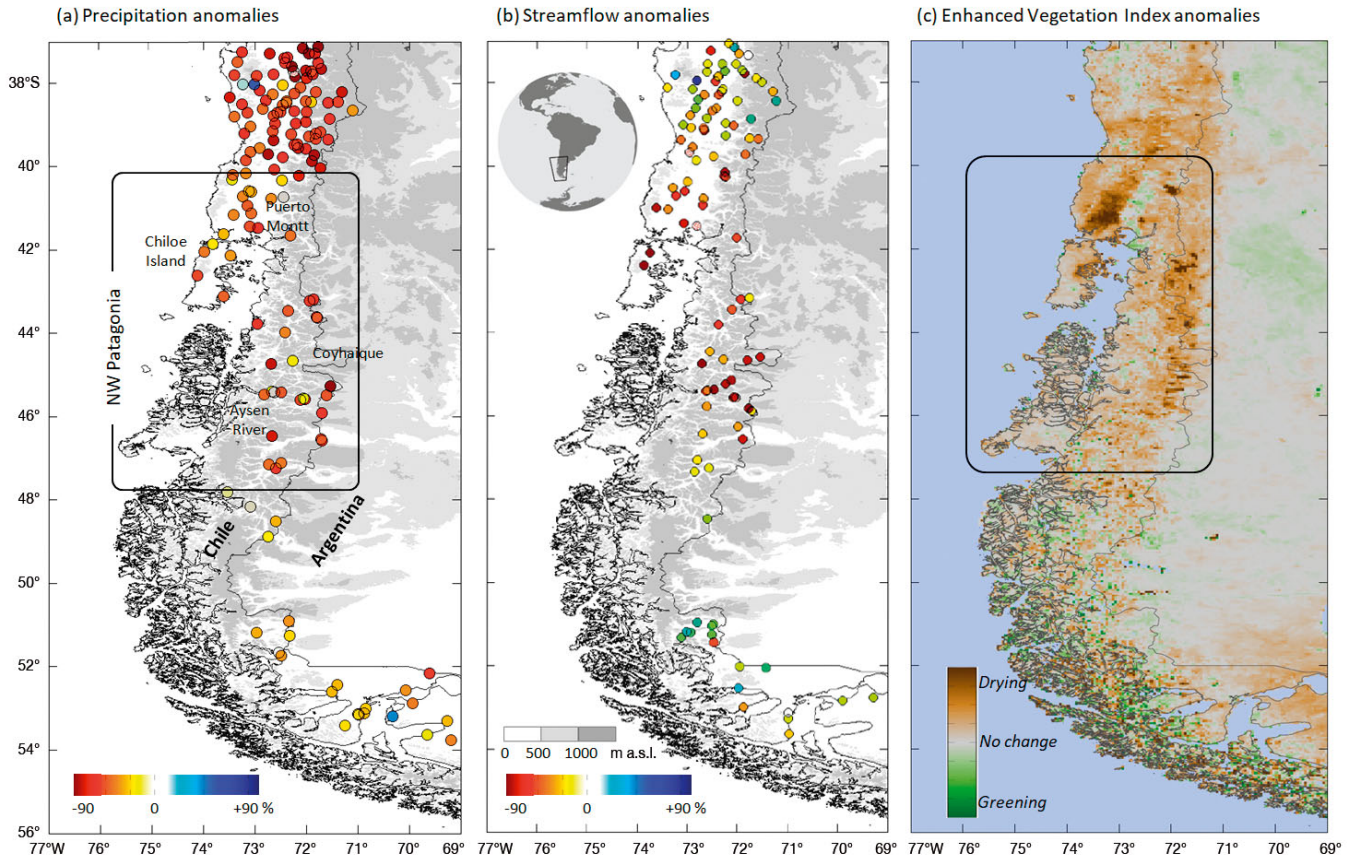


Fig. 1. (a) Topographic map of Patagonia (see (b) for elevation scale), delimitation of its northwestern sector (black box); key geographic features and accumulated rainfall anomaly (colored circles; percentage relative to 1980–2010) during January, February, March (JFM) 2016. (b) As in (a) but for stream flow anomalies. (c) MODIS-derived enhanced vegetation index anomalies during JFM 2016

mented in southern South America, nor have their tangible environmental impacts.

Local records and tree-ring based reconstructions (Garreaud et al. 2013, Muñoz et al. 2016) reveal a decrease in precipitation and streamflow in western Patagonia during the last 3–4 decades, particularly marked in summer and fall, associated with changes in the SH extratropical circulation (Garreaud et al. 2013). The latter has been linked to stratospheric ozone (O_3) depletion and the increase in greenhouse gas (GHG) atmospheric concentrations (Gillett & Thompson 2003, Arblaster & Meehl 2006), implying that this drying trend will persist, during the rest of the 21st century, with potentially detrimental effects on the environment.

Contributing to the drying trend, western Patagonia experienced its most severe drought on record during the first half of 2016, when rainfall and streamflow were half (or less) of their seasonal averages (Figs. 1a,b & 2d). In Section 3 of this work, we document the evolution, spatial extent, and return period of this drought, largely driven by precipitation

deficit. Subsequently (Section 4), we describe the large-scale climate anomalies that affected western Patagonia during 2016, causing the drought, and interpret them as the superposition of climate modes in their extreme phases. The dry conditions had detrimental impacts on vegetation and, as qualitatively discussed in Section 5, set the stage for multiple environmental disruptions. In late summer and fall (January to April 2016) a bloom of *Pseudochattonella* sp. and *Alexandrium catenella* caused the worst mass mortality of fish and shellfish ever recorded (including 10% of the Chilean salmon production) in the inner waters of Patagonia (Hernandez et al. 2016), and the so-called red tide extended abnormally along the Pacific coast from the Aysen region (ca. 45° S) to 39° S (Buschmann et al. 2016), generating considerable social, economic, and sanitary problems in Patagonia (Clément et al. 2016). Likewise, aggravated by the use of firewood for heat, the concentration of particulate matter was so high that the World Health Organization named Coyhaique, the capital of Aysen, the most polluted city in

the Americas during May 2016. The number of forest fires in Northern Patagonia in 2016 was also larger than during the average fire season. Given the extraordinary character of the 2016 precipitation deficit in Patagonia, the potential repetition of such conditions in the near future and the seemingly related environmental disruptions, the aim of this work was to explore local- and large-scale aspects of this drought, including its causes and selected impacts.

In addition to the climate forcing, local-scale impacts driven by human activities (population growth, aquaculture development, and native forest substitution by exotic species) likely played a role in the 2016 environmental crisis in Patagonia by increasing the vulnerability of the affected sectors to climate extremes (e.g. Miserendino et al. 2011, Buschmann et al. 2009, Iriarte et al. 2010). Disentangling the role of natural (e.g. ENSO) and anthropogenic (either local or remote) factors on environmental changes is fundamental if one wishes to make informed projections of the regional future. While such a task is beyond the scope of this work, addressing the climate forcing of extreme dryness (and possibly environmental extremes) in Patagonia is an important first step and can offer insights relevant to other west coast extra-tropical settings.

2. DATA

I used monthly means of SLP, downward flux of shortwave radiation at the surface, and wind components at selected pressure levels from the National Centers for Environmental Prediction (NCEP)–National Center for Atmospheric Research (NCAR) reanalysis (NNR; Kalnay et al. 1996) available from 1948 onwards on a $2.5 \times 2.5^\circ$ lat–long grid. It has been found that NNR has problems representing the SH circulation before the satellite era (i.e. before 1979; e.g. Tennant 2004), so the long-term means were calculated using the period 1980–2010. For selected fields, I further verified the hemispheric anomalies using the European Centre for Medium-Range Weather Forecasts (ECMWF) reanalysis (ERA-interim; Dee et al. 2011). Global precipitation was obtained from the Climate Prediction Centre (CPC) merged analysis of precipitation (CMAP; Xie & Arkin 1997) from 1979 onwards on a $2.5 \times 2.5^\circ$ lat–long grid. Sea surface temperature (SST) was obtained from NOAA high-resolution blended SST (Reynolds et al. 2007) from 1981 onwards on a $0.25 \times 0.25^\circ$ lat–long grid. Local-scale conditions were char-

acterized using daily records from 65 rain gauges and 12 river-flow stations in southern Chile ($38\text{--}56^\circ\text{S}$) operated by the Chilean Weather Service and Chilean Water Agency (obtained from the Chilean Climate Explorer; <http://explorador.cr2.cl/>), and daily mean concentration of PM₁₀ (airborne particulate matter of $<10\text{ }\mu\text{m}$) in Coyaique from the National Air Quality Information Service (SINCA 2016). I also employed high-resolution, MODIS-derived fields of enhanced vegetation index (Jiang et al. 2008) and chlorophyll *a* (chl *a*) (O'Reilly et al. 2000).

In addition to the observed dataset, I used a 30-member ensemble with the Max Plank Institute for Meteorology Model (ECHAM5.4) (Roeckner et al. 2003). ECHAM5.4 was integrated from January 1959 to April 2016 at $0.75 \times 0.75^\circ$ lat–long resolution, forced by observed SST and sea ice concentration (SIC) (Hurrell et al. 2008) and time-varying GHG and O₃. This simulation is referred to as AMIP-ORF (Atmospheric Modeling Intercomparison Project–observed radiative forcing), from the NOAA Facility for Climate Assessments (<https://www.esrl.noaa.gov/psd/repository/alias/facts/>).

3. THE 2016 SEVERE DROUGHT

Station-based seasonal rainfall anomalies for summer 2016 are shown in Fig. 1a and for other seasons in Fig. S2 in the Supplement at www.int-res.com/articles/suppl/c074p217_supp.pdf. A moderately wet winter 2015 (June, July, August, September; JJAS) was followed by a substantially dry spring and early summer, with rainfall deficits $>50\%$ between $40\text{--}47^\circ\text{S}$. The metrological drought intensified (rainfall deficits up to 90%) and expanded north and south during summer, and continued strong into fall and winter. Recall here that western Patagonia receives, on average, between 3000 and 9000 mm of precipitation more or less uniformly distributed throughout the year, so that a 50% deficit during summer–fall represents an actual shortage of several hundred mm, accounted by many days with little or no precipitation over an otherwise hyper-humid region. On the other hand, potential evapotranspiration is low over western Patagonia (owing to its temperate, maritime climate), so that precipitation deficit is the main driver of drought in this region. Indeed, both the standardized precipitation evapotranspiration index (SPEI; Vicente-Serrano et al. 2010) and reanalysis surface soil moisture anomalies indicate drought conditions in summer–fall 2016 across northwestern Patagonia (data not shown). Furthermore, the deficit

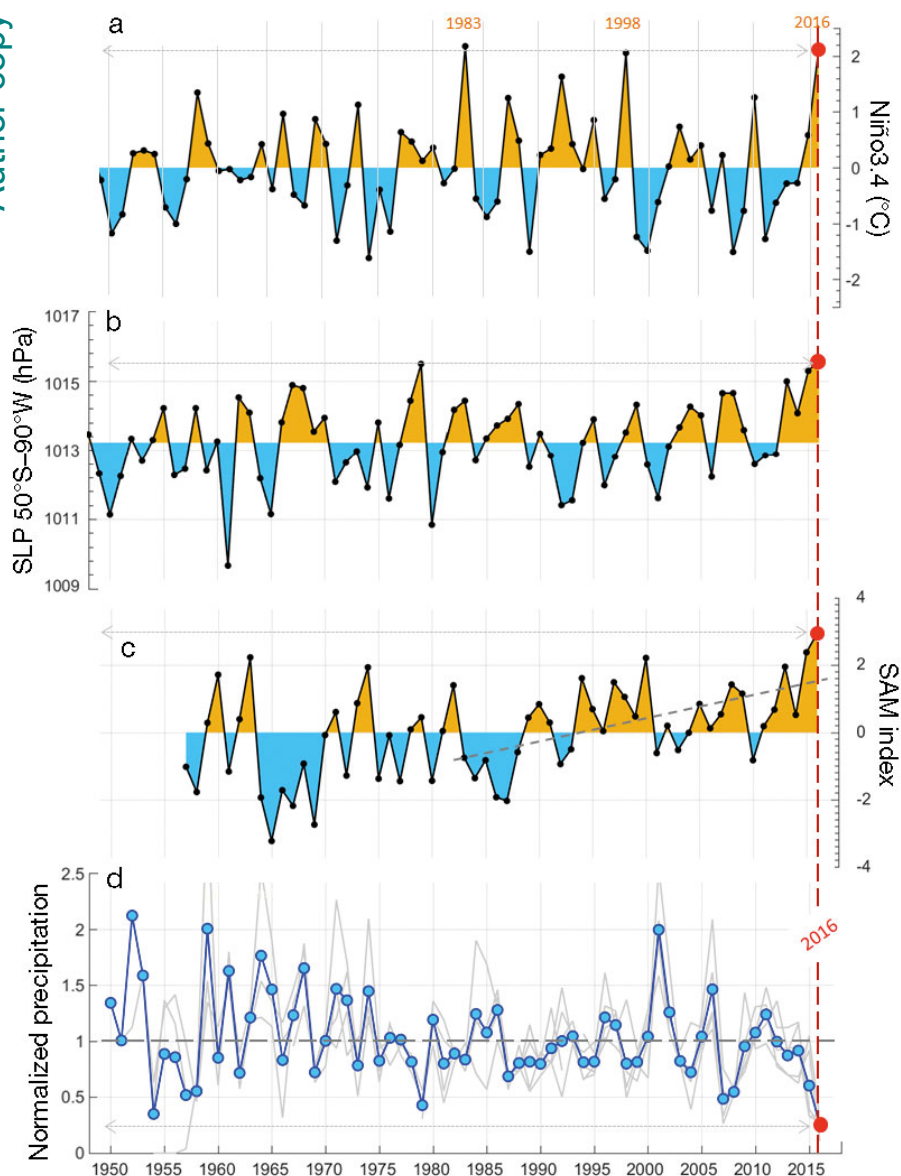


Fig. 2. The extreme summer of 2016 as shown by time series of selected variables (January, February, March [JFM] averaged). (a) Niño3.4 index from the Hadley Centre sea surface temperature data set HadISST1. (b) Sea level pressure (SLP) at 50° S, 90° W. (c) Southern Annular Mode (SAM) index as in Marshall (2003). (d) Blue line: CMAP precipitation over NW Patagonia (see Fig. 1). Grey lines: 3 individual stations in Patagonia (Puerto Montt, Aysen and Coyhaique). The precipitation series were divided by their long-term mean

of precipitation since spring 2015 seems to have had a detrimental impact on vegetation as revealed by the anomaly of the MODIS-derived enhanced vegetation index (EVI) during summer 2016. There is a widespread drying over western Patagonia, most notable along the western slope of the Andes and over inland valleys north of 42° S (Fig. 1c). Yet there are areas that have experienced greening (positive EVI anomalies) farther south, rendering a complex

vegetation response to precipitation deficit (e.g. Vicente-Serrano et al. 2013).

Given the relatively small size of the basins draining western Patagonia, the rainfall deficit leads to a concomitant decline in river discharge, and I found stream-flow anomalies ranging from –30 to –60 % relative to their long-term means (Fig. 1b). As an example, see Fig. 3a, which shows the daily discharge of the Aysen river. After the wet winter of 2015, the discharge dropped well below the historical lower quartile in October 2015 and, notably, reached record lows with the exception of a few modest floods.

Considering the rain gauge and river discharge records, SPEI data, re-analysis soil moisture and vegetation response, it is clear that the meteorological drought in early 2016 over western Patagonia rapidly transitioned into a hydrological and agriculture drought. To place the 2016 drought in context, Fig. 2d shows the time series of summer–fall precipitation at 5 stations across western Patagonia with relatively long records. Consistent with previous studies, there is a discernible drying trend since ca. 1960 that has been partially attributed to anthropogenic forcing (GHG, O_3) mediated by changes in the SH extratropical circulation (Gillett & Thompson 2003, Arblaster & Meehl 2006). The 2016 value stands out as the lowest rainfall accumulation in the last 67 yr; fitting a generalized extreme value probability distribution (GEV pdf) to the 1950–2005 data (thus excluding the last 10 yr) in individual stations results in a return period of 100 ± 20 yr for the 2016 drought.

The inferred lack of mid-latitude storms crossing the region had other meteorological manifestations that will be important when considering the environmental disruptions during early 2016. The time series of solar radiation reaching the surface over Patagonia (Fig. 3b) reveals almost uninterrupted positive anomalies from October 2015 to April 2016, summing nearly to a 20% increase in insolation. On the other hand, I also found a prevalence of cold conditions,

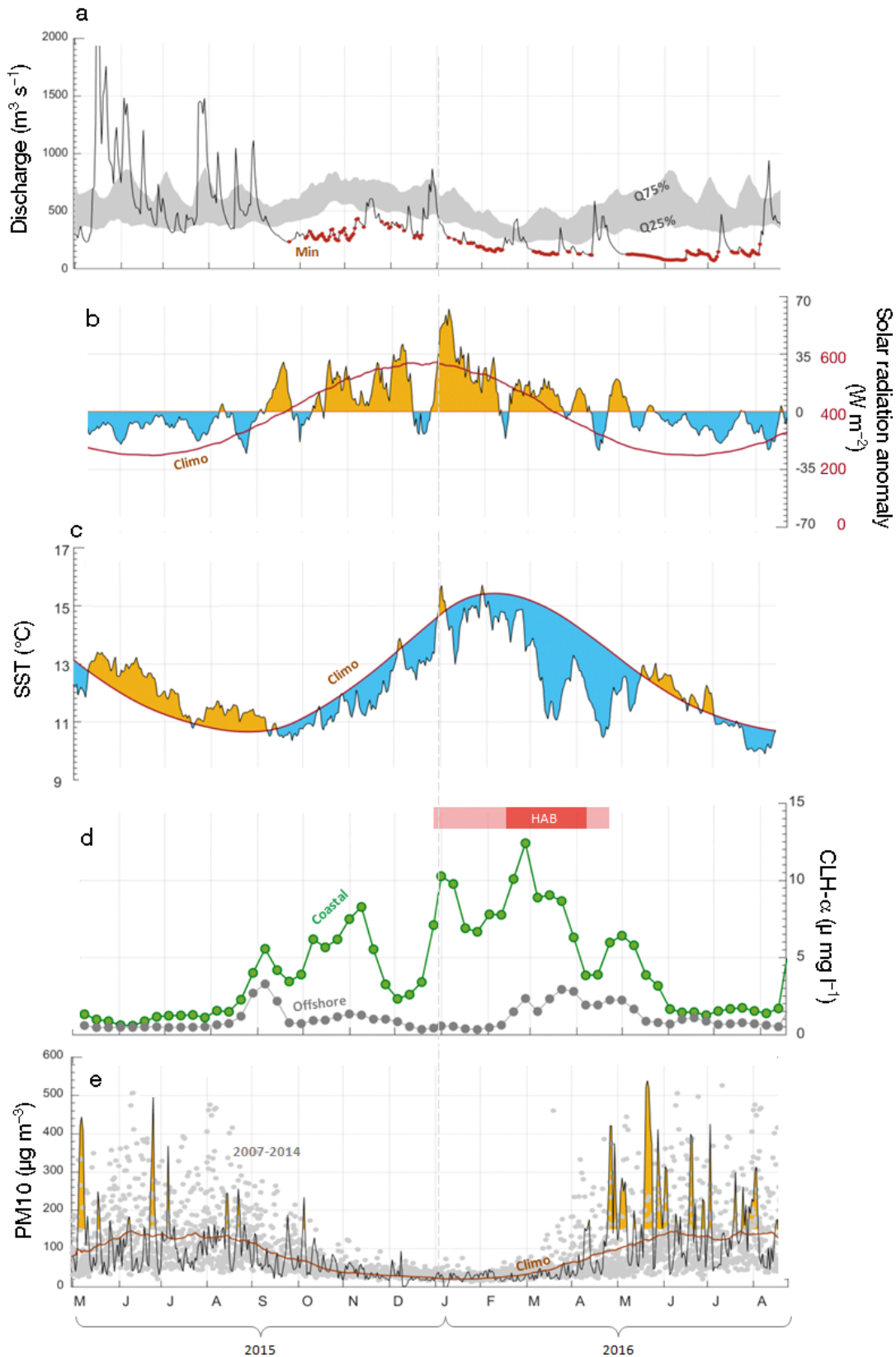


Fig. 3. Local environmental conditions over Patagonia during 2015–2016. (a) Daily mean discharge of the Aysen River (45.4°S , 72.6°W ; 23 m a.s.l.). Grey shading bounded by the historical (1995–2014) lower and upper quartiles; red dots indicate when last year values were the historical low. (b) 7 d running mean of daily surface solar radiation anomalies over NP; 'Climo' line: solar radiation long-term mean (scale shown in red); (c) 7 d running mean of daily sea surface temperature (SST) about 30 km off Chiloe (42.5°S , 74.3°W); 'Climo' line: SST long-term mean, (d) MODIS OC-3 8 d chlorophyll (CLH) concentration in a coastal (42.5°S , 74.3°W) and offshore box (42.5°S , 75.3°W); (e) daily mean concentration of airborne particulate matter of $<10 \mu\text{m}$ (PM10) in Coyaique. Orange area highlights PM10 values exceeding the Chilean norm; grey circles are historical daily values (2007–2014 'Climo' line: PM10 long-term mean)

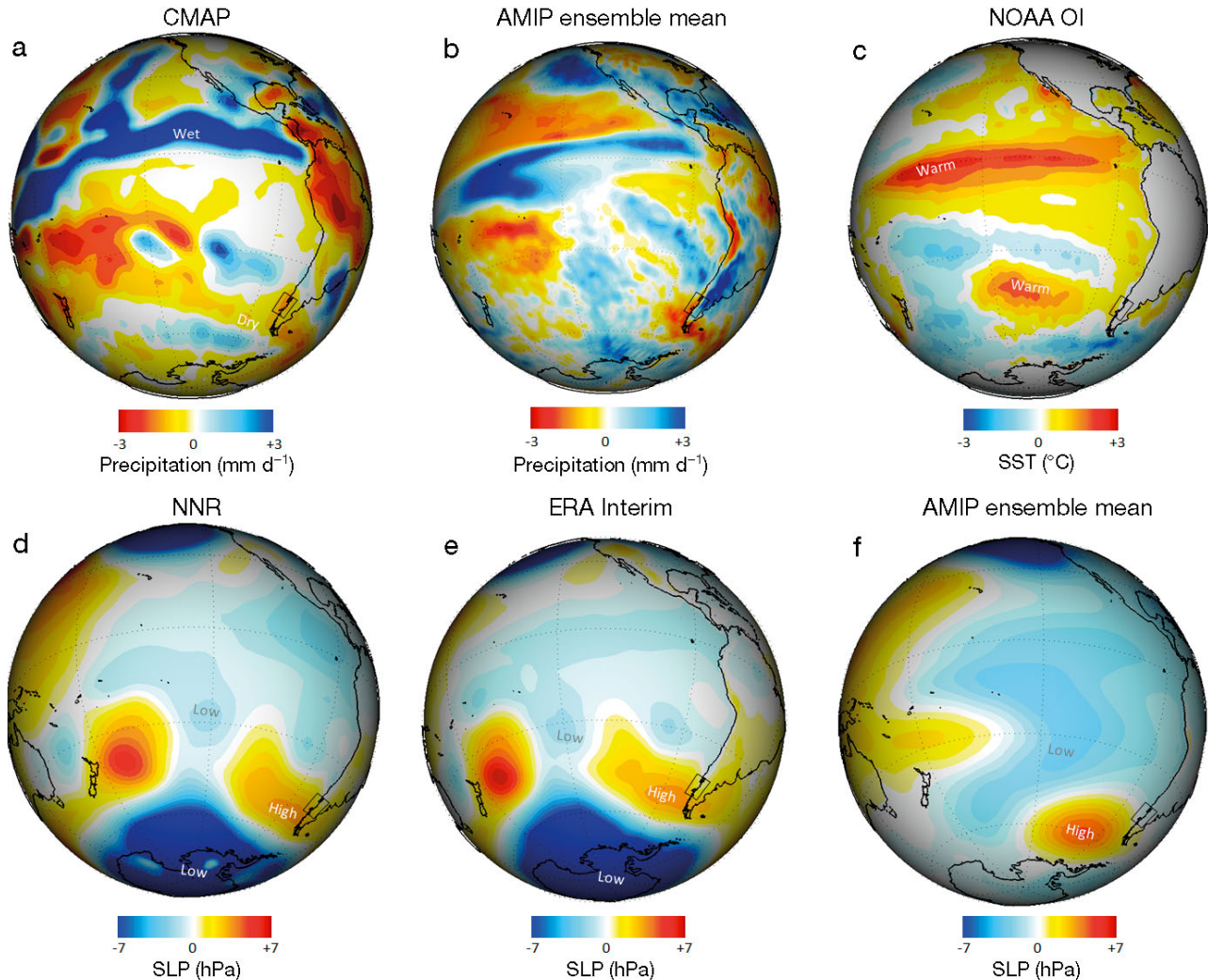


Fig. 4. Large-scale context during austral summer (JFM) 2016. (a) Observed (CMAP) precipitation anomalies; (b) ensemble mean precipitation anomalies from a 30 member ensemble ECHAM5.4 AMIP simulation (see Section 2 for details); (c) sea surface temperature anomalies; (d) observed (NCEP-NCAR Reanalysis) sea level pressure (SLP) anomalies; (e) observed (ERA-interim) SLP anomalies; (f) ensemble mean SLP anomalies from a 30 member ensemble ECHAM5.4 AMIP simulation. Black rectangles indicate the location of northwest Patagonia

particularly notable in the minimum (nighttime) temperatures, across western Patagonia from April to June 2016 (data not shown).

4. LARGE-SCALE ANOMALIES

As seen in global precipitation products, the drought in Patagonia was connected with a drier than average region that extended over much of the south Pacific (Fig. 4a). During the summer of 2016 (January, February, March; JFM) the SLP anomaly field exhibited a dipole over the SE Pacific, with negative values at low latitudes and positive values farther south (Fig. 4d,e). Large negative SLP anomalies

(>4 hPa) were found over the Antarctic. Off the continent at 50°S, the positive anomalies were among the largest on record (Fig. 2b) and greatly intensified the southern edge of the subtropical Pacific anticyclone, thus blocking the storm track and weakening the low- and mid-level westerly winds (Fig. 5, Fig. S1 in the Supplement). Since wind variability accounts for about 70% of the variance of rainfall at interannual time scales (Garreaud 2007, Garreaud et al. 2013), the wind anomalies largely explain the Patagonia drought in summer–fall 2016.

The intense anticyclone straddling austral Chile also created a steep pressure gradient force pointing northward along the coast of southern Chile, fostering equatorward, upwelling favorable surface winds

(Fig. S1) (Muñoz & Garreaud 2005). Indeed, I found upwelling-favorable wind events from October 2015 to March 2016 (Figs. S1 & S3 in the Supplement) off Chiloe island (ca. 42.5°S) where the climatological meridional wind is slightly negative (that is, mostly northerly, down welling favorable winds). I now relate these large-scale climate anomalies to the leading modes of atmospheric variability in the SH.

4.1. ENSO forcing

From 2011 through 2013, cold conditions prevailed in the tropical Pacific until a rapid warming began in late 2014 leading to a strong El Niño event by mid-2015 (Bell et al. 2017). The Niño3.4 index (the most influential for central-southern Chile climate; Montecinos & Aceituno 2003) reached +3°C in December 2015 and the average value for austral summer 2016 was +2°C (Fig. 2a), the second largest on record since 1948. Indeed, the seasonal anomaly maps of SST, SLP and precipitation (Figs. 4c,d,e) do show features typical of an El Niño event, somewhat closer to the Central Pacific events (e.g. Capotondi et al. 2015). The warming across the tropical Pacific excited quasi-stationary Rossby waves that contributed to the ridging off southern South America (Karoly 1989, Renwick 1998) and the weakening of the zonal flow impinging Patagonia. In the summer of 2016, the Rossby wave was evident in the 200 hPa geopotential height anomalies (see Fig. S4 in the Supplement), with persistent centers of positive anomalies off the equator in the central Pacific, negative anomalies in the subtropics and a third center of positive anomalies at higher latitudes to the west of the southern tip of the continent. The latter is directly above the positive SLP anomalies in Fig. 4d, indicative of the barotropic character of these perturbations. This observed arrangement is in qualitative agreement with results from simple numerical modeling forced by tropical heating (Bladé & Hartmann 1995)

During summer, Niño3.4 accounts for about one-third of the interannual variance of the zonal wind at 850 hPa over western Patagonia (U850). The power of the fit was tested using the general linear F -statistics (from the regression analysis of variance) whose p -value is <0.05 . I used a linear fit to calculate the ENSO-congruent U850 anomaly for 2016 obtaining 7.7 m s^{-1} , about 60% of the observed anomaly (Fig. 5). The uncertainty in the regression coefficients was employed to estimate the uncertainty in the ENSO-congruent U850, emphasizing the partial role of ENSO in weakening the flow over Patagonia

(Fig. 5). Similar results were found when using SLP as the predicted variable, lending statistical support to the prominent role of El Niño in forcing the observed large-scale anomalies in southern South America.

Further evidence for the role of ENSO is provided by results from the ECHAM5.4 AMIP simulations. Since the ensemble members are forced by identical boundary conditions and only differ in slightly different initial conditions, the ensemble mean isolates the SST-forced response of the atmospheric circulation under current levels of radiative forcing. Fig. 4f shows the ensemble mean SLP anomalies during JFM 2016, which are in close correspondence with their observed counterpart (Figs. 4d,e) over much of the Pacific (spatial correlation coefficient $r = 0.69$ in the region 10°N–50°S, 180–60°W). Of particular relevance, the simulated anticyclonic ensemble mean anomalies off southern South America are located in the same place as the observed anomalies with an intensity slightly stronger than observed. The simulated zonal wind at 850 hPa and precipitation anomalies over Patagonia are also in good agreement with the observations (Fig. 4b for precipitation; for the wind field the spatial correlation coefficient between the observed and simulated fields reach 0.57 in the region 10°N–50°S, 180–60°W). Nonetheless, dispersion among ensemble members is large, with 20% of the members producing a wet summer in Patagonia, indicative of the important role of internal variability in shaping the seasonal anomalies. Within the modeling framework, internal variability represents the aggregated effect of transient, synoptic-scale events, not forced by the underlying SST but dependent on the initial conditions.

El Niño was capable of warming most of the SE Pacific, but coastal conditions differed from the broader behavior as illustrated by the time series of SST in a grid box about 30 km off Chiloe Island (Figs. 3c & S3). Slightly cold anomalies appeared by September 2015 and increased gradually during late spring and early summer. Local SST then experienced a marked cooling in March and April 2016 (2.5°C colder than average) followed by a rapid recovery by the end of May.

4.2. SAM forcing and combined effects

During summer 2016, the nearly circumpolar dipole in the mass field between mostly positive anomalies in mid-latitudes and very negative anomalies at high latitudes (Fig. 4d,e) strongly resembled the

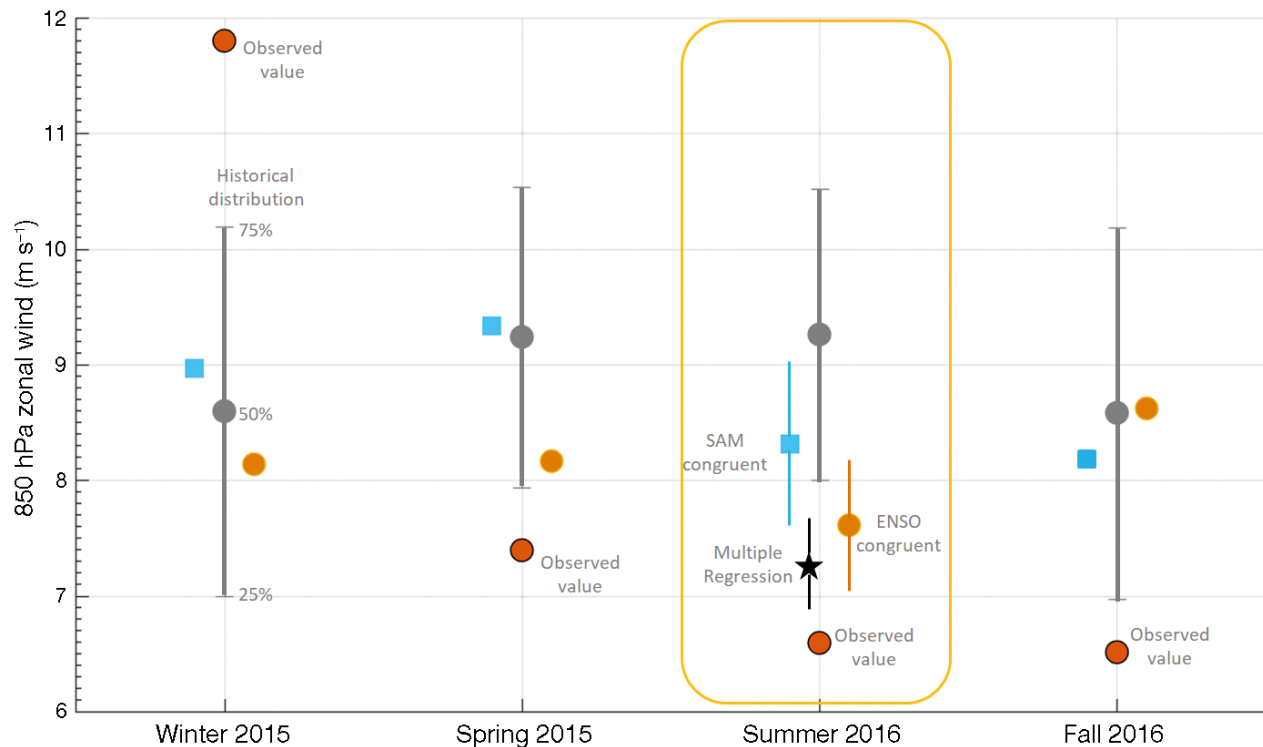


Fig. 5. Historical distribution of the seasonal mean 850 hPa zonal wind (U850) over western Patagonia (45°S, 75°W) from NCEP-NCAR reanalysis (1948–2014). The distribution is shown by the whiskers with extremes at 25 and 75 % percentiles and the grey circle (50 % percentile). Also shown are the values observed in 2015–2016 (red circles) as well the El Niño–Southern Oscillation (ENSO)-congruent (orange circles) and Southern Annular Mode (SAM)-congruent (blue squares). For the summer 2016 the black star is the value of U850 predicted by multiple regression using Niño3.4 and SAM indices. The errors bars in the X-congruent values are a measure of the regression uncertainty; see Section 4.1 for the definition of the X-congruent values

SAM pattern, and the positive SAM index (Marshall 2003) was the highest on record (Fig. 2c). To assess the role of SAM on the climate anomalies of Patagonia, I also perform a linear regression between SAM index and U850. During austral summer, SAM explains ~25% of the interannual variance of U850 (still significant, with an F -statistics p -value < 0.1), and the SAM-congruent value for 2016 is 8.2 m s^{-1} (Fig. 5), a low value in the historical context but not as low as observed (6.6 m s^{-1}).

What caused the extreme high SAM during the summer of 2016? The ensemble mean of the ECHAM5.4 AMIP simulations have a very weak signal over Antarctic (Fig. 4f), suggesting that the surface ocean played little role (if any) in forcing the pressure anomalies at high latitudes (and hence the overall SAM signal). On the other hand, the positive SAM value during JFM 2016 (as well as the values in the last 5 summers) fits well with the trend toward a positive polarity since the mid-1970s. Note, however, that the extremely high SAM index in 2016 stands out well above the value predicted by the trend (dashed line in Fig. 2c), suggesting again an impor-

tant role of internal variability (i.e. synoptic-scale transients not related to external or boundary-condition forcings; Limpasuvan & Hartmann 1999). The recent SAM trend is very robust (e.g. Thompson & Wallace 2000, Marshall 2003, Jones et al. 2016) and stands out when compared against tree-ring multi-centennial reconstructions (Lara et al. 2008, Villalba et al. 2012). Likewise, the summer SAM positive trend simulated by CMIP-5 fully-coupled historical climate simulations exceeds the 95% level of control variability (Jones et al. 2016) consistent with the expected effects of stratospheric O_3 depletion and, to a lesser extent, increased GHG concentrations (Gillett & Thompson 2003, Arblaster & Meehl 2006, Gillett et al. 2013).

Recent studies (L'Heureux & Thompson 2006, Ding et al. 2012, Wang & Cai 2013) have found that ENSO and SAM are not independent. The connection arises, at least partially, because warm SST anomalies in the tropical Pacific during El Niño years are capable of forcing Rossby wave trains, with one of its anticyclone nodes over the Amundsen-Bellingshausen Sea in the Antarctic periphery (Mo & Higgins

1998, Renwick 1998) favoring a negative polarity of SAM (i.e. positive pressure anomalies at higher latitudes). Thus, a negative association has been found between Niño3.4 and SAM indices, although the strength of their correlation varies at seasonal and decadal time scales (Yu et al. 2015). During austral summer, the correlation is rather weak ($r_{\text{[SAM index; Niño3.4]}} = -0.12$; F -statistics $p < 0.2$) as evident in the scatterplot of both indices in Fig. 6. Consistently, the amount of variance of U850 accounted for by a multiple linear regression using both indices rises to nearly 50 % (F -statistics $p = 0.01$), and the predicted seasonal anomaly for the summer of 2016 is 7.2 m s^{-1} , much closer to the observed anomaly than using individual regressions (Fig. 5).

The fact that both ENSO and SAM were in their positive phases during the summer of 2016 is rather puzzling, considering their overall negative correlation (Fig. 6). In this case, however, the ridging induced by the ocean forcing maximized at 60°S (to the north of the Amundsen-Bellingshausen Sea) and extended well into mid-latitudes (Fig. 4f) where the SAM-related belt of anticyclonic anomalies is typically located. I thus posit that SAM provided an important circulation background (positive SLP anomalies at mid-latitudes) upon which the strong ENSO-related anomalies were superimposed as to produce the marked ridging off austral Chile and hence the extreme dry conditions over Patagonia.

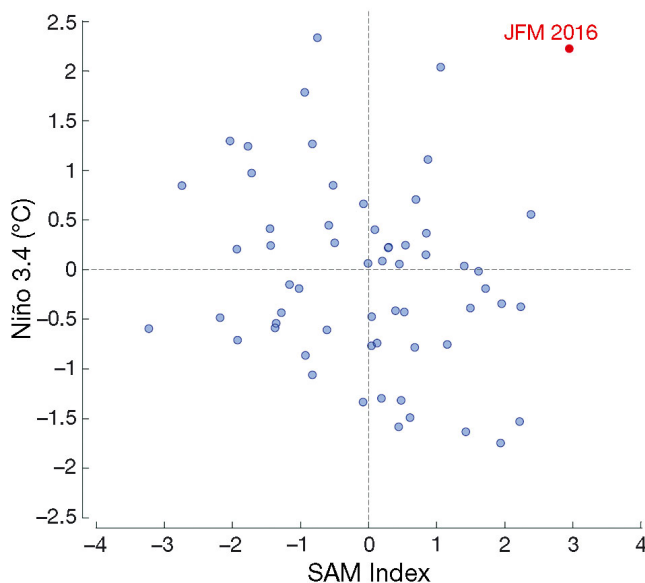


Fig. 6. Austral summer (January, February, March; JFM) values of the Niño3.4 and Southern Annular Mode (SAM) indices (as in Marshall 2003). Data from 1957–2016; values from 2016 are highlighted in red

4.3. Seasonal variations

I have focused my analysis on the summer of 2016 because the large-scale anomalies reached extreme values and the unprecedented drought/HAB took place in that season. Anomalous climate conditions, however, began before and persisted after summer (e.g. Fig. 5) as shown by the seasonal mean of zonal wind at 850 hPa over western Patagonia (U850). Stronger than average westerlies prevailed during the winter of 2015 (May, June, July, August) but transitioned to weaker flow in spring. The seasonal mean U850 reached a minimum in summer 2016 and low values persisted into fall. Consistently, the observed SLP anomalies in that season show a very intense blocking anticyclone centered over the southern tip of the continent (see Fig. S5 in the Supplement).

As shown in Fig. 3a, ENSO-congruent values of U850 were also low in spring 2015 and summer 2016, but near average in winter 2015 (because of a weak correlation between U850 and Niño3.4) and fall 2016 (because of the weakening of El Niño). Moreover, the ensemble mean of the ECHAM5.4 AMIP simulations for this season fails to capture the position and intensity of the anticyclonic anomalies over Patagonia (Fig. S5). Likewise, the SAM-congruent U850 anomalies were only significant in summer 2016. This suggests that the superposition of the ENSO and SAM forcing on Patagonia climate anomalies was important in summer 2016 and, to a lesser extent, in the previous season. Conversely, internal variability played a more prominent role in maintaining the climate anomalies over Patagonia during fall and winter 2016.

5. DISCUSSION AND OUTLOOK

Marked anticyclonic anomalies off southern South America and weak westerly flow impinging the austral Andes persisted from late spring 2015 to fall 2016, reaching record-breaking values at the height of the summer (JFM). These large-scale conditions resulted in the most intense drought on record ($>50\%$ precipitation deficits) in western Patagonia as well as excessive ($>30\%$) solar radiation reaching the surface, and frequent southerly, upwelling-favorable winds along the coast where northerly winds generally prevail. Although specific diagnostic studies are required, these regional anomalies were, very likely, important ingredients for the severe air pollution episodes, major forest fires, and the worst recorded HAB in Patagonia. Here, I speculate on the connec-

tion between the aforementioned meteorological anomalies and the environmental disturbances in western Patagonia during the first half of 2016.

(1) *Augmented forest fire activity.* Both the number of forest fires and the area burned during the fire season 2015–2016 (July–June) in the Chilean Lake district and Aysen region (coincident with northwestern Patagonia) were about 15 % larger than their historical counterparts (CONAF 2017), including some major fires (over 200 ha) in late summer of 2016. Most forest fires in central Chile are human-ignited but their propagation (and final burned area) are largely dictated by atmospheric variables (Holz & Veblen 2012). In particular, the burned area in southern Chile is well correlated with summer rainfall and temperature, so the extreme meteorological drought in early 2016 (and the concomitant drying of the vegetation; Fig. 1) seems an important driver of the augmented fire activity in that season.

(2) *Acute urban air pollution.* Between April and June 2016, the daily values of PM₁₀ measured in Coyhaique (ca. 50 000 inhabitants) persisted well above the long-term mean, reaching values as high as 500 $\mu\text{g m}^{-3}$ and exceeding the Chilean norm (PM₁₀ < 150 $\mu\text{g m}^{-3}$) more than half of the time (Fig. 3e). As in other urban centers in Chile, variations in air quality in Coyhaique are largely controlled by changes in atmospheric ventilation rather than by changes in emissions (Rutllant & Garreaud 1995, UNTEC 2015). Although we do not have local wind data, the lack of rainfall during fall signals reduced low-level flow and more stagnant atmospheric conditions, which, coupled with colder than normal nights, resulted in poor ventilation and the acute, protracted urban air pollution reported in Coyhaique. The air pollutants were mainly emitted by firewood used for heating during winter (UNTEC 2015); the previously reported forest fires occurred earlier (summer months) and farther away from urban areas.

(3) *The worse ever recorded HAB.* A long-lasting (January–April 2016; Fig. 3d) and spatially extended (45–39° S) HAB (*Pseudochattonella* sp. and *Alexandrium catenella*) afflicted the inner and offshore waters of northern Patagonia (IFOP 2016) causing a massive mass mortality of fish and shellfish, with major social and economic impacts (Hernandez et al. 2016). The biophysical causes of this HAB are complex and currently under scrutiny (Buschmann et al. 2016, Hernandez et al. 2016). Normally, large freshwater inputs (direct rainfall and river discharge) lead to stratification of the coastal water column (León-Muñoz et al. 2013, Iriarte et al. 2016) limiting nutrient exchanges between the surface layer (mainly fresh

and brackish water) and deep layers (mainly from oceanic origin). Consequently, inorganic nutrients and radiation are considered limiting factors for high primary productivity in these systems (González et al. 2013). The drought in western Patagonia substantially reduced the freshwater input and weakened the vertical stratification in the inner waters of Patagonia, thus increasing the upward intrusion of saline, nutrient-rich waters into the surface layer (León-Muñoz et al. 2018). Unusual southerly winds offshore also contributed to more frequent upwelling of nutrient-rich, oceanic water masses. Under these altered hydro-biological conditions, the heightened solar radiation reaching the surface provided optimal conditions for the algal bloom (León-Muñoz et al. 2018).

The large-scale climate anomalies were, in turn, mostly forced by the strong El Niño-related atmospheric teleconnections superimposed on the positive phase of the SAM. The ENSO forcing points to an opportunity for seasonal prediction of environmental disturbances in Patagonia, although limited by the role of internal (non-deterministic) variability. The SAM forcing, on the other hand, allows us to put this year's drought in context and to assess its recurrence in the future. Since during the positive phase of SAM the westerlies weaken around 40° S, precipitation decreases and temperature increases over western Patagonia (e.g. Gillett et al. 2006, Garreaud et al. 2009). Thus, the summertime drying trend in western Patagonia over the last 4 decades (Aravena & Luckman 2009, Quintana & Aceituno 2012) has been attributed to the SAM positive trend, which, in turn, is forced by stratospheric O₃ depletion and increased GHG concentrations (Gillett & Thompson 2003, Arblaster & Meehl 2006). The connection among O₃ depletion, GHG increase and Patagonia drying has been explicitly shown by Gonzalez et al. (2014).

The role of climate change in drying Patagonia can be directly assessed by considering the results from a pool of 104 CMIP-5 fully coupled simulations generated by 26 models in support of IPCC-AR5 (Collins et al. 2013). The number of members per model ranges from 1 to 10. Simulated rainfall anomalies during summer (November to March) over western Patagonia for the period 2010–2020 under the RCP8.5 scenario range from –3 to –16 % (with respect to 1970–2000), with a multi-model, multi-ensemble mean (i.e. the anthropogenic forced response) of –7 %. Thus, global climate change has already reduced precipitation in Patagonia, although the extreme drought in summer 2016 (50–60 % rainfall deficit) was further sustained by a strong ENSO forcing and internal ('weather noise') variability.

Dryer than present conditions are also consistently projected for northwestern Patagonia towards the end of the century under high GHG emission scenarios (Collins et al. 2013), as the increase in GHG concentration will continue to shift the SH storm track poleward (Yin 2005, Chang et al. 2012) and SAM toward its positive polarity (Arblaster et al. 2011, Zheng et al. 2013, Morgenstern et al. 2014). Superposition of El Niño events in this altered climate may result in a higher frequency of extreme dry summers and perhaps environmental disruptions as observed in 2016. The coming decades may experience an ease in the drying trend because the stratospheric O₃ recovery will transitorily weaken the SAM tendency towards its positive polarity (e.g. Barnes et al. 2014). At the same time, however, local human activities (e.g. aquaculture, timber, tourism) are rapidly increasing across Patagonia, altering the environmental functioning in this region.

Acknowledgements. This study received financial support from CONICYT (Chile) through the FONDAP Research Center (CR)2 (15110009). Dr. José Rullant provided constructive comments on the manuscript. An updated rain gauge and river streamflow data set were provided by the Chilean agencies DGA and DMC, and is available at www.cr2.cl. Air pollution data for Coyaique from 'Sistema de Información Nacional de Calidad del Aire' is available at <http://sinca.mma.gob.cl/>. NNR, CMAP and SST fields, as well as Niño3.4 and SAM indices, were obtained from the Physical Division of the NOAA Earth System Research Laboratory at www.esrl.noaa.gov/psd/. The ensemble of AMIP-ECHAM5.4 is available at <http://www.esrl.noaa.gov/psd/repository/alias/facts/>. Chlorophyll concentration 8 d fields from NASA's OceanColor Web: <https://oceancolor.gsfc.nasa.gov/> and EVI from the MODIS land-surface team are available at <https://modis.gsfc.nasa.gov/data/dataproduct/mod13.php>.

LITERATURE CITED

- ✦ Aravena JC, Luckman BH (2009) Spatio-temporal rainfall patterns in southern South America. *Int J Climatol* 29: 2106–2120
- ✦ Arblaster JM, Meehl GA (2006) Contributions of external forcings to Southern Annular Mode trends. *J Clim* 19: 2896–2905
- ✦ Arblaster J, Meehl G, Karoly D (2011) Future climate change in the Southern Hemisphere: competing effects of ozone and greenhouse gases. *Geophys Res Lett* 38:L02701
- ✦ Barnes EA, Barnes NW, Polvani LM (2014) Delayed Southern Hemisphere climate change induced by stratospheric ozone recovery, as projected by the CMIP5 models. *J Clim* 27:852–867
- Bell G, L'Heureux M, Halpert MS (2017) ENSO and the tropical Pacific. *Bull Am Meteorol Soc* 98:S93–S98
- ✦ Bladé I, Hartmann DL (1995) The linear and nonlinear extra-tropical response of the atmosphere to tropical intra-seasonal heating. *J Atmos Sci* 52:4448–4471
- ✦ Buschmann AH, Cabello F, Young K, Carvajal J, Varela DA, Henríquez L (2009) Salmon aquaculture and coastal ecosystem health in Chile: analysis of regulations, environmental impacts and bioremediation systems. *Ocean Coast Manage* 52:243–249
- Buschmann AH, Farias L, Tapia F, Varela D, Vasquez M (2016) Scientific report on the 2016 southern Chile red tide. Chilean Department of Economy. www.academiadeciencias.cl/wp-content/uploads/201704infofinal_comisionmarearoja_21nov2016-pdf/
- ✦ Capotondi A, Wittenberg AT, Newman M, Di Lorenzo E and others (2015) Understanding ENSO diversity. *Bull Am Meteorol Soc* 96:921–938
- ✦ Chang EK, Guo Y, Xia X (2012) CMIP5 multimodel ensemble projection of storm track change under global warming. *J Geophys Res D Atmospheres* 117:D23118
- Clément A, Lincoqueo L, Saldiva M, Brito CG and others (2016) Exceptional summer conditions and HABs of *Pseudochattonella* in southern Chile create record impacts on salmon farms. *Harmful Algae News* 53:1–3
- Collins M, Knutti R, Arblaster J, Dufresne JL and others (2013) Long-term climate change: projections, commitments and irreversibility. In: Stocker TF, Qin D, Plattner GK, Tignor MMB and others (eds) *Climate change 2013: the physical science basis. Contribution of Working Group I to the Fifth Assessment Report of the Intergovernmental Panel on Climate Change*. Cambridge University Press, Cambridge, p 1029–1136
- CONAF (Corporación Nacional Forestal) (2017) Compendio Estadístico Ocurrencia y Daño Incendios Forestales 1985–2016. Corporación Nacional Forestal, Santiago
- ✦ Dee DP, Uppala S, Simmons A, Berrisford P and others (2011) The ERA-interim reanalysis: configuration and performance of the data assimilation system. *QJR Meteorol Soc* 137:553–597
- ✦ Ding Q, Steig EJ, Battisti DS, Wallace JM (2012) Influence of the tropics on the Southern Annular Mode. *J Clim* 25: 6330–6348
- ✦ Garreaud RD (2007) Precipitation and circulation covariability in the extratropics. *J Clim* 20:4789–4797
- ✦ Garreaud R, Vuille M, Compagnucci R, Marengo J (2009) Present-day South American climate. *Palaeogeogr Palaeoclimatol Palaeoecol* 281:180–195
- ✦ Garreaud R, Lopez P, Minvielle M, Rojas M (2013) Large-scale control on the Patagonian climate. *J Clim* 26: 215–230
- ✦ Gillett NP, Thompson DWJ (2003) Simulation of recent Southern Hemisphere climate change. *Science* 302: 273–275
- ✦ Gillett N, Kell T, Jones P (2006) Regional climate impacts of the Southern Annular Mode. *Geophys Res Lett* 33: L23704
- ✦ Gillett NP, Fyfe JC, Parker DE (2013) Attribution of observed sea level pressure trends to greenhouse gas, aerosol, and ozone changes. *Geophys Res Lett* 40:2302–2306
- ✦ González HE, Castro LR, Daneri G, Iriarte JL and others (2013) Land-ocean gradient in haline stratification and its effects on plankton dynamics and trophic carbon fluxes in Chilean Patagonian fjords (47–50°S). *Prog Oceanogr* 119:32–47
- ✦ Gonzalez PL, Polvani LM, Seager R, Correa GJ (2014) Stratospheric ozone depletion: a key driver of recent precipitation trends in south eastern South America. *Clim Dyn* 42:1775–1792

- Hernández C, Díaz P, Molinet C, Seguel M (2016) Exceptional climate anomalies and northwards expansion of paralytic shellfish poisoning outbreaks in Southern Chile. *Harmful Algae News* 54:1–3
- ✦ Holz A, Veblen TT (2012) Wildfire activity in rainforests in western Patagonia linked to the Southern Annular Mode. *Int J Wildland Fire* 21:114–126
- ✦ Hurrell JW, Hack JJ, Shea D, Caron JM, Rosinski J (2008) A new sea surface temperature and sea ice boundary dataset for the community atmosphere model. *J Clim* 21: 5145–5153
- IFOP (2016) Red tide monitoring project. Instituto Chileno de Fomento Pesquero. <https://www.ifop.cl/marearaja/>
- ✦ Iriarte JL, González HE, Nahuelhual L (2010) Patagonian fjord ecosystems in southern Chile as a highly vulnerable region: problems and needs. *Ambio* 39:463–466
- Iriarte JL, León-Muñoz J, Marcé R, Clément A, Lara C (2016) Influence of seasonal freshwater streamflow regimes on phytoplankton blooms in a Patagonian fjord. *NZJ Mar Freshw Res* 51:304–315
- ✦ Jiang Z, Huete AR, Didan K, Miura T (2008) Development of a two-band enhanced vegetation index without a blue band. *Remote Sens Environ* 112:3833–3845
- ✦ Jones JM, Gille ST, Goosse H, Abram NJ and others (2016) Assessing recent trends in high-latitude Southern Hemisphere surface climate. *Nat Clim Chang* 6:917–926
- Kalnay E, Kanamitsu M, Kistler R, Collins W and others (1996) The NCEP/NCAR 40-Year Reanalysis Project. *Bull Am Meteorol Soc* 77:437–471
- ✦ Karoly DJ (1989) Southern Hemisphere circulation features associated with El Niño–Southern Oscillation events. *J Clim* 2:1239–1252
- ✦ L'Heureux ML, Thompson DW (2006) Observed relationships between the El Niño–Southern Oscillation and the extratropical zonal-mean circulation. *J Clim* 19:276–287
- ✦ Lara A, Villalba R, Urrutia R (2008) A 400-year tree-ring record of the Puelo River summer–fall streamflow in the Valdivian Rainforest eco-region, Chile. *Clim Change* 86: 331–356
- ✦ Lara C, Saldías GS, Tapia FJ, Iriarte JL, Broitman BR (2016) Interannual variability in temporal patterns of chlorophyll-*a* and their potential influence on the supply of mussel larvae to inner waters in northern Patagonia (41–44° S). *J Mar Syst* 155:11–18
- ✦ León-Muñoz J, Marcé R, Iriarte J (2013) Influence of hydrological regime of an Andean river on salinity, temperature and oxygen in a Patagonia fjord, Chile. *NZJ Mar Freshw Res* 47:515–528
- León-Muñoz J, Urbina M, Garreaud R, Iriarte JL (2018) Hydroclimatic conditions trigger record harmful algal bloom in western Patagonia (summer 2016). *Sci Rep* 8: 1330
- ✦ Limpasuvan V, Hartmann DL (1999) Eddies and the annular modes of climate variability. *Geophys Res Lett* 26: 3133–3136
- ✦ Marshall GJ (2003) Trends in the Southern Annular Mode from observations and reanalyses. *J Clim* 16:4134–4143
- ✦ Martínez-Harms MJ, Gajardo R (2008) Ecosystem value in the western Patagonia protected areas. *J Nat Conserv* 16:72–87
- ✦ Miserendino ML, Casaux R, Archangelsky M, Di Prinzio CY, Brand C, Kutschker AM (2011) Assessing land-use effects on water quality, in-stream habitat, riparian ecosystems and biodiversity in Patagonian northwest streams. *Sci Total Environ* 409:612–624
- ✦ Mo K, Higgins R (1998) The Pacific–South American modes and tropical convection during the Southern Hemisphere winter. *Mon Weather Review* 126:1581–1596
- ✦ Montecinos A, Aceituno P (2003) Seasonality of the ENSO-related rainfall variability in central Chile and associated circulation anomalies. *J Clim* 16:281–296
- ✦ Montecinos A, Kurgansky MV, Muñoz C, Takahashi K (2011) Non-ENSO interannual rainfall variability in central Chile during austral winter. *Theor Appl Climatol* 106:557–568
- ✦ Morgenstern O, Zeng G, Dean SM, Joshi M, Abraham NL, Osprey A (2014) Direct and ozone mediated forcing of the Southern Annular Mode by greenhouse gases. *Geophys Res Lett* 41:9050–9057
- ✦ Muñoz RC, Garreaud R (2005) Dynamics of the low-level jet off the west coast of subtropical South America. *Mon Weather Rev* 133:3661–3677
- ✦ Muñoz AA, González-Reyes A, Lara A, Sauchyn D and others (2016) Streamflow variability in the Chilean Temperate-Mediterranean climate transition (35°S–42°S) during the last 400 years inferred from tree-ring records. *Clim Dyn* 47:4051–4066
- O'Reilly JE, Maritorena S, O'Brien MC, Siegel DA and others (2000) SeaWiFS postlaunch calibration and validation analyses, Part 3. In: Hooker SB, Firestone ER (eds) *SeaWiFS postlaunch technical report series, Vol 11*. NASA/TM2002-206892, NASA Center for Aerospace Information, Hanover, MD
- Paruelo JM, Beltran A, Jobbagy E, Sala OE, Golluscio RA (1998) The climate of Patagonia: general patterns and controls on biotic. *Ecol Austral* 8:85–101
- Quintana J, Aceituno P (2012) Changes in the rainfall regime along the extratropical west coast of South America (Chile): 30–43°S. *Atmosfera* 25:1–22
- ✦ Renwick JA (1998) ENSO-related variability in the frequency of South Pacific blocking. *Mon Weather Rev* 126: 3117–3123
- ✦ Reynolds R, Smith T, Liu C, Chelton D, Casey K, Schlax M (2007) Daily high-resolution-blended analyses for sea surface temperature. *J Clim* 20:5473–5496
- Roeckner E, Bäuml G, Bonaventura L, Brokopf R and others (2003) The atmospheric general circulation model ECHAM 5. I. Model description. Max Planck Institute for Meteorology, Hamburg
- ✦ Rutllant J, Garreaud R (1995) Meteorological air pollution potential for Santiago, Chile: towards an objective episode forecasting. *Environ Monit Assess* 34:223–244
- ✦ Schneider C, Gies D (2004) Effects of El Niño–Southern Oscillation on southernmost South America precipitation at 53°S revealed from NCEP–NCAR reanalyses and weather station data. *Int J Climatol* 24:1057–1076
- ✦ Silvestri G, Vera C (2009) Nonstationary impacts of the Southern Annular Mode on Southern Hemisphere climate. *J Clim* 22:6142–6148
- SINCA (Servicio de Informacion Nacional de Calidad del Aire) (2016) Online and historical air pollution information in Chile. <http://sinca.mma.gob.cl/index.php/region/index/id/XI>
- ✦ Smith RB, Evans JP (2007) Orographic precipitation and water vapor fractionation over the southern Andes. *J Hydrometeorol* 8:3–19
- ✦ Tennant W (2004) Considerations when using pre-1979 NCEP/NCAR reanalyses in the southern hemisphere. *Geophys Res Lett* 31:L11112
- ✦ Thompson DW, Wallace JM (2000) Annular modes in the

- extratropical circulation. I. Month-to-month variability. *J Clim* 13:1000–1016
- UNTEC (2015) Characterization of the air pollution meteorological potential in the Aysen region, Chile. Technical report prepared by the Foundation for Technological Transfer (UNTEC), Santiago
- ✦ Viale M, Garreaud R (2015) Orographic effects of the subtropical and extratropical Andes on upwind precipitating clouds. *J Geophys Res Atmos* 120:4962–4974
- Vicente-Serrano S, Beguería S, López-Moreno J (2010) A multiscalar drought index sensitive to global warming: the standardized precipitation evapotranspiration index. *J Clim* 23:1696–1718
- ✦ Vicente-Serrano SM, Gouveia C, Camarero JJ, Beguería S and others (2013) Response of vegetation to drought time-scales across global land biomes. *Proc Natl Acad Sci USA* 110:52–57
- ✦ Villalba R, Lara A, Masiokas MH, Urrutia R and others (2012) Unusual Southern Hemisphere tree growth patterns induced by changes in the Southern Annular Mode. *Nat Geosci* 5:793–798
- ✦ Wang G, Cai W (2013) Climate-change impact on the 20th-century relationship between the Southern Annular Mode and global mean temperature. *Sci Rep* 3:2039
- ✦ Xie P, Arkin P (1997) Global precipitation: a 17-year monthly analysis based on gauge observations, satellite estimates, and numerical model outputs. *Bull Am Meteorol Soc* 78: 2539–2558
- ✦ Yin JH (2005) A consistent poleward shift of the storm tracks in simulations of 21st century climate. *Geophys Res Lett* 32:L18701
- ✦ Yu JY, Paek H, Saltzman ES, Lee T (2015) The early 1990s change in ENSO–PSA–SAM relationships and its impact on Southern Hemisphere climate. *J Clim* 28: 9393–9408
- ✦ Zheng F, Li J, Clark RT, Nnamchi HC (2013) Simulation and projection of the Southern Hemisphere annular mode in CMIP5 models. *J Clim* 26:9860–9879

*Editorial responsibility: Ricardo Trigo,
Lisbon, Portugal*

*Submitted: April 18, 2017; Accepted: December 5, 2017
Proofs received from author(s): January 24, 2018*